View metadata, citation and similar papers at core.ac.uk

brought to you by CORE

provided by Digital Repository @ Iowa State University

IOWA STATE UNIVERSITY
Digital Repository

Graduate Theses and Dissertations

Iowa State University Capstones, Theses and Dissertations

2016

Gasification of liquid sprays in an entrained flow gasifier

Nicholas Ryan Creager
Iowa State University

Follow this and additional works at: https://lib.dr.iastate.edu/etd


Part of the Mechanical Engineering Commons

Recommended Citation
Creager, Nicholas Ryan, "Gasification of liquid sprays in an entrained flow gasifier" (2016). *Graduate Theses and Dissertations*. 15140.
https://lib.dr.iastate.edu/etd/15140

This Thesis is brought to you for free and open access by the Iowa State University Capstones, Theses and Dissertations at Iowa State University Digital Repository. It has been accepted for inclusion in Graduate Theses and Dissertations by an authorized administrator of Iowa State University Digital Repository. For more information, please contact digirep@iastate.edu.

Gasification of liquid sprays in an entrained flow gasifier

by

Nick Creager

A thesis submitted to the graduate faculty

in partial fulfillment of the requirements for the degree of

MASTER OF SCIENCE

Major: Mechanical Engineering

Program of Study Committee:
Robert C. Brown, Major Professor
Song-Charng Kong
Steven J. Hoff

Iowa State University

Ames, Iowa

2016

TABLE OF CONTENTS

TABLE OF FIGURES

TABLE OF TABLES

ACKNOWLEDGEMENTS

First, a thank you to God whom has given me an abounding life full of opportunity and wonder. Second, to my gracious wife, Julianne, and my immediate family Bryce, Jane, Adam and Mindy; who has stood by my side with encouragement throughout all of my studies. Third, to my Program of Study committee who provided this unique project to me to further my engineering skills and expertise under their guiding eye. Finally, to my friends and co-worker who's help and support made this project possible.

ABSTRACT

In an advancing technological world, gasification is a relatively mature technology that can be refreshed to help achieve sustainable energy production. This thesis discusses the development of a pressurized gasification system that converts bio-oil from fast pyrolysis of red oak into producer gas. Focus will be given to the challenges of operating a pressurized system at high temperature while injecting a non-uniform liquid. Demonstration experiments using methanol resulted in development of experimental methods to show critical nozzle designs and their affects on gasification of liquid jets.

Start up of the bio-oil gasification system was performed using methanol as a model fuel. Methanol provides a stable platform for proving the system's capabilities and focused attention on areas that needed design improvements. The ideal fuel also made it easy to compare the system results directly with theoretical calculations of equilibrium. The methanol experiments highlighted a need to show the importance of volatility verses the importance of atomization. Due to this discovery, the experiments where adjusted to demonstrate the change in atomization within a fixed system.

Producing the whole bio-oil that 1) could be readily pumped 2) would not clog the system and 3) have congruent properties throughout testing proved to be a challenge within itself. A list of lab experiments were conducted to show differences in bio-oils that had been filtered to three difference sizes; 500µm, 90µm and 40µm. To best show the importance in atomization, the 90µm bio-oil was selected. The bio-oil gasification tests were performed using 3 nozzle configurations. Each nozzle showed a unique result while further proving that atomization is critical to performing gasification of liquid jets.

CHAPTER 1 INTRODUCTION

Gasification systems for fuel synthesis or gas turbine-based power generation are ideally operated at high pressures. Feeding solid feedstocks into pressurized gasifiers requires complicated lock hoppers or other mechanical systems that are expensive and often unreliable. In contrast, liquids are easily pumped into pressurized systems. Hydrophilic solids like coal can be pulverized and mixed with water to form pumpable slurries. This is not possible with hydrophilic solids like most biomass. Pyrolysis of biomass produces a liquid product, better known as bio-oil, that can be easily transported and pumped to high pressures using existing liquid handling systems. [1]

The goal of this research was to construct and demonstrate a bio-oil gasification system. The system design was developed for pressures up to 700 psi_g with temperatures as high as 1000^oC while maintaining adiabatic experimental conditions. Focus was given to the filtration and quantification of whole bio-oil, while reactor testing coordinated around the effects of gasification on liquid jets.

CHAPTER 2 BACKGROUND

Gasification is a process in which a material containing carbon and hydrogen is thermally broken down in to two main gas components, carbon monoxide (CO) and hydrogen (H_2), the combination of these two gases is known as synthesis gas or syngas. Gasification can be thought of as partial combustion of the feedstock. Typically, gasification occurs between 20 to 40% of oxygen for a stiochiometric burn of the fuel. The temperature range for gasification is between 700^{o}C to 1500^{o}C depending on the type of gasifier and the feedstock being used. [2]

In the 1800's, syngas was generated using coal to provide towns with gas lighting. Due to the discovery of readily available natural gas and petroleum products, the production of syngas gradually waned. In World War II, due to the petroleum shortage, syngas was once again produced to supplement the energy usage of vehicles and industrial machinery. When the war ended the demand for petroleum decreased and gasification was discontinued for transportation purposes. [3]

Due to a worldwide push for sustainable and environmentally friendly fuels, gasification is once again being considered as a way of producing power. Conventional fuels for gasification are coal and natural gas, but these are not the only substances that can be gasified. Any organic compound can be gasified. Therefore, this is a great way to produce fuels from what are considered to be carbon neutral sources. Carbon neutral sources do admit carbon, but the amount emitted is counteracted by the amount of carbon sequestered throughout the feedstock's life span. [5] Examples of carbon neutral organic compound are wood, cornstover, switchgrass, or miscanthus. [2]

Syngas is a desirable fuel because of its versatility in producing other fuels. Syngas can be used as a stand-alone fuel for a variety of uses, such as electrical power production or heating. It can also be upgraded to produce hydrogen. Additionally, methanol, a chemical that is used frequently as fuels for heat engines and other industrial applications, is synthesized from syngas. Through Fischer-Tropsch synthesis, syngas can be converted to higher molecular weight carbon chain fuels such as gasoline and diesel. [4]

There are several different types of gasifiers in operation today, but they can be combined into three categories: entrained flow, fixed bed, and moving bed. In each of the three categories are two variations of

the particular type of gasifier. Each variation of gasifier has distinct features that provide advantages and disadvantages to its design. [2]

2.1 Fixed Bed

Fixed bed reactors contain multiple levels of reaction zones and the order of the reaction zones depends on whether the gasifier is a downdraft or updraft reactor. The updraft reactor has the feedstock entering in from the top of the reactor, the feedstock then piles up to form the fixed bed. Air is introduced to the system below the fixed bed and then travels up through the feedstock resulting in the reaction zones, as shown in Figure 1. These reaction zones will be described in more detail later in this paper. For downdraft fixed bed gasifiers, the air travels in the same directions as the feedstocks as seen in Figure 2. The result of this change affects where the reaction zones occur in the fixed bed gasifier. In both cases the ash falls through the fixed bed for collection at the bottom of the reactor when the feedstock is fully reacted. The fixed bed gasifiers are the oldest and simplest type of gasifiers in operation and generally operate at temperatures between 800^{o}C and 1200^{o}C. [4]

2.2 Fluidized Beds

Fluidized bed gasifiers consist of bubbling fluidized beds and circulating fluidized beds. Fluidized bed reactors operate at lower temperature than fixed bed and entrained flow gasifiers due to the increase in heat uniformity and high heat transfer rates due to the feedstock's direct interaction with the bed material. The bed materials are made of small uniform particles of sand or alumina. Consequently, the temperature cannot get too high or the bed material and ash will start to agglomerate; therefore, fluidized bed gasifiers operate in the 700^{o}C to 1000^{o}C temperature range. Oxygen, air, steam or a combination of these components are typically used to fluidize the bed. The gases are introduced below the bed and as they travel upwards they cause the sand or alumina to act like a fluid for which feedstocks can be passed into. [4]

2.3 Entrained Flow

Entrained flow gasifiers transport fine particles or droplets of the feedstock in a gas stream that moves through the reactor. There are two types of entrained flow gasifiers: slagging and non-slagging. These two types are differentiated by their operating temperatures. Typically, a non-slagging gasifier will operate between 700°C and 1000°C. This is when the ash particles will remain in a solid state and a majority can be collected by the filtration cyclones with any char that is formed in the system. The slagging gasifier generally operates between 1250°C to 1500°C. At these temperatures the ash in the system will melt and collect on the walls of the reactor where they flow to the bottom and exit as a molten slag. [6]

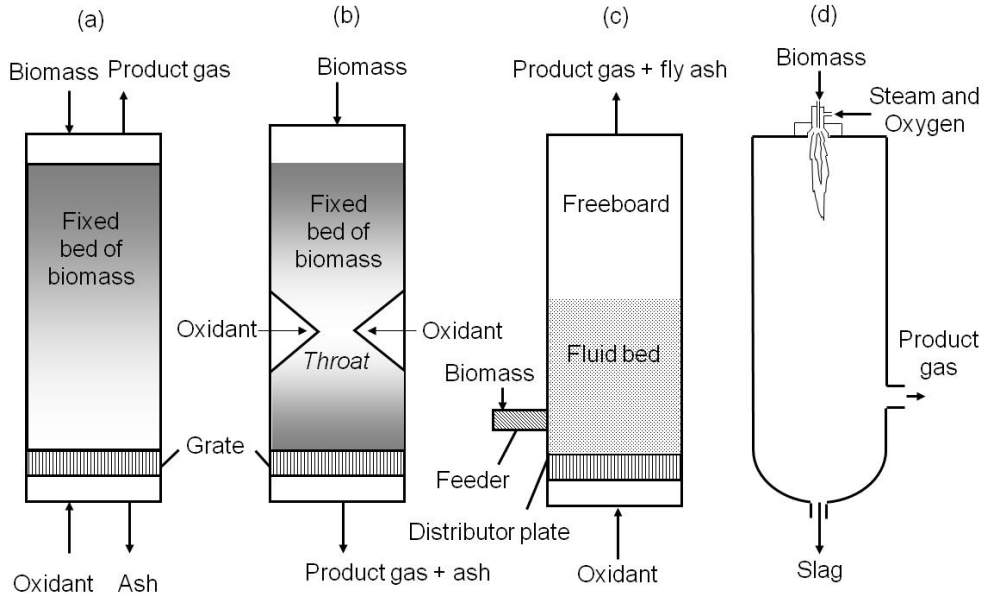

Figure 1 Pictorials of Aforementioned Gasifiers: a) Updraft, b) Downdraft, c) Fluidized Bed, and d) Entrained Flow [2]

Table 1 Types of Gasifiers

	Advantages	Disadvantages
Updraft fixed bed	• Low setup and operation cost • Can handle high moisture content feedstocks • Mature and reliable technology	• Requires extensive hot gas cleanup to remove tars
Downdraft fixed bed	• Low setup and operation cost • High tar removal • Mature and reliable technology	• Requires low moisture feedstocks • Low thermal efficiency
Bubbling fluidized bed	• High heat transfer rates • Very uniform heat distribution • Can handle a variety of feedstock sizes	• High gas flow rates can allow feedstocks to bypass the bed • Limited temperature range
Circulating fluidized bed	• High heat transfer rates • Good uniform heat distribution • Can handle a variety of feedstock sizes	• Limited temperature range • Temperature gradients can occur in the direction of solid flow
Slagging entrained flow	• High temperature range • High feedstock conversion rates • Low tar production • Liquefied ash	• Expensive set up • High energy consumption
Non-slagging entrained flow	• High feedstock conversion • Low tar production • Low set up cost	• Requires small particle sizes

2.4 Gasification process:

There are four main stages that a feedstock, such as biomass, transitions through during gasification. The first is the drying stage. This can occur in the gasifier or before the biomass is fed into the reactor. During this stage the water and light organic acids are removed from the biomass, which happens at low temperature between 100^{o}C and 200^{o}C. The next stage is pyrolysis. Pyrolysis occurs when the biomass reaches temperatures between 300^{o}C and 500^{o}C but there is little or no oxygen available for the biomass to react with. In this temperature range the biomass will emit large quantities of tars and gases such as carbon monoxide, hydrogen, and carbon dioxide. The third and forth stages can occur in different sequences depending on where and how the oxygen is being supplied to the gasifier. The third stage is gas-solid reactions, which includes the following reactions: [3]

$$C + CO_2 = 2CO$$
$$C + H_2O = CO + H_2$$
$$C + 2H_2 = CH_4$$
$$C + O_2 = CO_2$$

The fourth stage is gas-phase reactions:[3]

$$CO + H_2O = CO + H_2$$
$$CO_2 + H_2 = CO + H_2O$$
$$2H_2 + O_2 = 2H_2O$$

By introducing water into the system instead of oxygen the gasifier becomes a steam reformer. [7] Many times steam is used in conjunction with air or oxygen gasifiers. The steam provides an environment that helps promote the water gas shift reaction that increases the yield of hydrogen being produced from the reactor. Along with steam, different catalysts are used to help control the reactions that take place in a gasifier. Most commonly used are nickel-based catalysts, but catalysts can be selected or created to assist in the production of desired products. Catalysts are also used after the gasification process to upgrade the syngas to usable fuels and chemicals such as methanol. [8]

Gasification of bio-based feedstocks provides a number of challenges, ranging from high oxygen content to high ash content. An example of biomass is cornstover, a byproduct of corn harvest. As corn is produced in large fields, the biomass needs to be collected and transported to a central location for processing. The transportation can be challenging due to the low density of biomass. Also, the low density makes economical storage difficult. Biomass can also contain high levels of moisture, which can be detrimental to the efficiency of a reactor. Additionally, due to the fibrous nature of the feedstock, the material can interlock with itself making the feedstock difficult to inject into a gasifier. [9] Due to the solid state of biomass, it becomes challenging to create a pressurized feeding system which is necessary to help push the syngas through downstream processes such as a hot gas cleanup system. Finally, biomass has a high content of inorganic minerals that can cause ash fouling. Generally, gasifiers will have two cyclone particle filters in series to filter out the majority of the inorganic minerals and unconverted char, but they are limited to 97-98% efficiency. [10]

2.5 Bio-oil Production:

Bio-oil is a product of fast pyrolysis. Bio-oil can have up to five times the energy density of the biomass from which it is produced, as shown by Figure 3. Pyrolysis reactors run at temperatures between 400°C and 600°C and can produce up to 70% of their original weight as oil. [11] The other 30% is split between non-condensable gases and biochar. Biochar is collected with gas cyclones. These collect up to 97-98% of the remaining solid particles left in the gas stream, the other 2-3% is condensed out with the bio-oil. Biochar is mostly organic carbon and can be sequestered for carbon credit or can be run through a gasifier to produce syngas and ash. [13] The bio-oil can be condensed out in two different fashions: all at once or as several fractions. By using an electrostatic precipitator (ESP) at constant temperature the aerosols can be electrically drawn out of the gas stream and into a liquid phase. Then the water and acids can be condensed out leaving only the non-condensable gas. If the water is removed separately from the aerosols, the heating value of the oil will increase. [14]

Figure 2 Bulk density between biomass (right) and bio-oil (left) [12]

2.6 Bio-oil Gasification:

Bio-oil gasification has several advantages over biomass gasification. Fast pyrolysis helps address costly transportation issues as the bio-oil has a much higher energy density than biomass. [11] Due to bio-oil being a liquid, it can be collected and stored in tanks easier than biomass; therefore, traditional transportation methods can be used. There are also fewer problems with feeding bio-oil over biomass.

Since pyrolysis converts the fibrous material into a liquid, the bio-oil can then be pumped into the reactor. With solid biomass, a series of pressurized lock hoppers would have to be used to maintain

continuous pressurized flow. A pressurized gasification reactor eliminates the need for expensive high volume compressors downstream of the gasifier. Consequently, the gas can be directly supplied at temperatures and pressures required for catalytic upgrading to liquids like methanol. The pyrolysis reactor also removes a large portion of the inorganic solid and char from the biomass. This in turn makes the syngas produced from the bio-oil cleaner than the gas produced directly from the biomass. [13]

Bio-oil gasification is limited to certain kinds of gasifiers. Updraft and downdraft gasifiers will not work with bio-oil. This is due to the air needing to pass through the feedstock. Bio-oil is a thick liquid and does not allow air to pass through easily like water, biomass, or sand. Therefore, bio-oil reactors are limited to fluidized beds and entrained flow gasification reactors. These reactors work well because the moving air, steam, or sand breaks up the bio-oil into small droplets, at which point the heat transfer through the bio-oil is very fast and vaporizes it before it can turn to coke, causing a clogging of the reactor. Bio-oil coking is not well understood but occurs when the oil is heated up over 100^{o}C at which time the oil starts to turn into a solid carbonaceous material. Coking is a problem in a bio-oil delivery system due to elevated temperatures. Bio-oil gasifiers can also handle bio-oil slurries. Slurries allow for solid partials to be mixed in with the bio-oil. Slurries can range from coal to biomass or the biochar produced during the fast pyrolysis process. [15]

Gasification of biomass in the presence of steam can produce high concentrations of hydrogen in the product gas. The University of British Columbia preformed a study on hydrogen production using a bubbling fluid bed reactor. Their results are found in Table 2. [16] Compared to gasification of solid biomass at Iowa State University (see Table 3), bio-oil gasification produces considerably more hydrogen, suggesting its use to produce renewable hydrogen.

Table 2 Bubbling fluidized bed gasification reactor results from University of British Columbia [16]

Reactor temperature, 800°C; on a dry N_2 free base; Values in mol%							
Bed Material	Feedstock	H_2	CO	CO_2	CH_4	C_2+	MJ- HHV/m^3
Sand	Bio-oil	35	33	13	11	4	15.8
	Slurry	39	28	16	10	2	12.4
Catalyst	Bio-oil	57	10	24	3	0	9.4
	Slurry	59	8	25	1	0	8.3

Table 3 Bubbling fluidized bed gasification reactor results from Iowa State University [17]

Reactor temperature, 800°C; on a dry N_2 free base; Values in mol%							
Bed Material	Feedstock	H_2	CO	CO_2	CH_4	C_2+	MJ- HHV/m^3
Sand	Biomass	20	28	35	10	4	11

CHAPTER 3 EXPERIMENTAL METHODS

3.1 Experimental Objective:

The objective of this project is to quantitatively evaluate the effects of high-pressure and varying equivalence ratios on bio-oil gasification. The parametric parameters will be evaluated qualitatively using: (1) overall carbon conversion efficiency via a system mass balance and (2) syngas quality by using a micro gas-chromatograph (micro GC).

3.2 Biomass to Bio-oil:

The biomass chosen for these experiments was red oak, due to its high oil yield and low ash content. The biomass was converted to bio-oil using an 8kg/h process development unit (PDU) pyrolyzer located at Iowa State University's BioCentury Research Farm (BCRF).

A super sack of red oak biomass is loaded into the main feed hopper using a forklift. The biomass is conveyed up into a system of two lock hoppers separated by knife gates. These gates allow the PDU to be operated in the absence of oxygen by purging the biomass with nitrogen. Two augers separate the hoppers from the pyrolysis reactor. The first meters the biomass at a constant 8kg/h by using an Acrison® weight metering system that continuously monitors the change in mass of the system to reliably supply material at a constant rate. The second auger rotates faster than the first to prevent pyrolysis reactions from starting before the biomass reaches the reactor bed.

The reactor is a bubbling fluidized bed, consisting of ASME 6-inch stainless steel nominal pipe size (NPS) with a schedule-40 wall thickness. The reactor is externally heated to 550^{o}C using Watlow® clamshell heaters. The bed material is pure silica sand and is sized to 600μm before it is placed inside the reactor. To maximize heat transfer and bed fluidization while minimizing sweep gas and heat loss, nitrogen gas is preheated using electrical star-wound cable heaters. Once the nitrogen gas is heated, it was passed through a distributing plate to fluidize the reactor bed.

Reactions in the biomass release non-condensable gases (NCG), volatile compounds, aerosols, and char particles. The nitrogen gas transports these products out of the fluid bed reactor and on to the

collections system. First, up to 95% of the char is removed using a system of two cyclone filters in series. Each of the cyclones are heated to 450°C to prevent condensation of volatiles. After the cyclones, there are a series of stages consisting each of a condenser and an electrostatic precipitator (ESP) to remove volatile compounds and aerosols respectively. The ISU system uses three stages reducing the temperature in each stage to collect different compounds resulting in six separate bio-oil fractions. The Iowa State University's process development pyrolyzer is shown in figure 3. The stages are known as stage fractions (SF) 1-6. The remaining condensable compounds and aerosols are collected using packed bed with glass wool as the media. A slip stream of the NCGs are removed to be analyzed by a micro GC. The remaining gas stream is sent to a reducing flare.

Figure 3 Iowa State University Bubbling Fluidized Bed Pyrolysis Process Development Unit

3.3 Bio-oil mixing:

Immediately after the six fractions were collected, SF 1-3 were placed in an oven at 80°C for 30 minutes to maintain a reduced viscosity and to maintain a homogeneous mixture prior to mixing all six fractions. The six fractions were poured into a 5 gallon bucket, partially submerged in steam water, and stirred for 10 minutes using a electric drill. Finally, the solution was poured over a 500 µm screen into a

second five gallon bucket to ensure no large chunks of the heavy fractions remained. The second five gallon bucket was then sealed and immediately refrigerated.

3.4 Bio-oil Filtration:

One liter of the 500µm filtered bio-oil was separated out and set aside for baseline testing. The remainder of the bio-oil was poured into a heated 316 stainless steel drum submerged in a heated water bath. The bio-oil was mixed using a three phase fully proportional motor as shown in figure 4. The bio-oil was heated and constantly stirred until the mixture reached 60^{o}C. The oil was extracted through electrically insulated stainless steel lines by a set of Teledyne 500D dual syringe pumps. The pumps provided a constant flow rate of 10mL/min to a 90µm inline pressure filter. The resulting filtered oil was then collected in one liter Nalgene® bottles. Two bottles of 90µm filtered bio-oil were randomly selected and filtered again through the same system, this time using a 40µm inline pressure filter.

Figure 4 Bio-oil mixing/filtration system

3.5 Bio-oil Gasification:

The bio-oil gasification system is composed of four subsystems; liquid feeding system, gasifier, gas cleanup, and gas analysis. The liquid feeding system supplies liquid feedstocks and gases needed for the

gasification process. The gasifier provides a high temperature environment via electrical heaters to promote and contain the gasification reactions. Following the gasification process, the gas cleanup system removes liquid contaminants from the syngas stream using stainless steel tubes in water jackets. The syngas is then sent to a Micro Gas Chromatograph for compositional gas analysis.

The liquid feeding system uses two 500mL dual feeding Teledyne® syringe pumps to inject liquid at precise flow rates. The stainless steel tubing of the feeding system is also wrapped with electrical heaters to pre-heat the feedstock to 60^{o}C to reduce viscosity and increase the fluid's pumpability. The liquid feedstock is then injected into the gasifier using an atomization nozzle. Pure oxygen or an oxygen/nitrogen mixture was metered using a Brooks mass flow meter. For the experiments the liquid fuel was injected at 10 mL/min and the gas flow was adjusted to maintain a stoichiometric balance of 25 percent. Stainless steel tubing was selected for its chemically resistive proprieties and resiliencies to bending, in addition to being readily accessible.

The nozzles were made from two concentric pieces of stainless steel tubing. The interior tube, measuring 0.125 inch OD and 0.055 inch ID, was used to transport the liquid feedstock to the end of the nozzle. The 0.125 inch tubing was tapered on one end at approximately 50 degrees. A set of perpendicular cuts were made on the tapered end of the nozzle so when the 0.125 inch tubing was seated against the exterior tubing, as shown in the Nozzle 3 view below, the oxygen still had a flow path. The exterior tubing was made from 0.25 inch OD and 0.018 inch wall thickness stainless steel tubing and provided a flow path for the oxygen gas to reach the nozzle exit. This exterior tubing needed to be modified to redirect the flow of oxygen directly over the exiting liquid fuel. The end of the 0.25 inch tube was welded shut then rounded over using a grinder into a hemisphere. A 0.1875 inch 135 degree drill bit was then used to ream out the inside of the 0.25 inch tubing. This drill bit was run down until it started to dent the welded face, but stopped before it broke through. Finally, a 0.0625 inch drill bit was used to place the final hole in the end of the exterior tubing.

Both the liquid feedstock and the oxygen gas interact at the end of the nozzle where the gas velocity enacts a shearing moment on the liquid feedstock driving the atomization of the fuel. Due to experimental results from shake down trials using methanol as the liquid feedstock, the focus of this work was atomization of the fuel within the gasifier. To do this, the 0.125 inch tubing carrying the bio-oil was moved up and down with respect to the end of the nozzle, thereby changing the gas orifice size. Figure 5 shows the three positions the nozzle was operated at in these experiments. Nozzle 1 was set so the bio-oil tube was not touching the outer shroud but the ends were flush with each other. On nozzle 2 the bio-oil tube was recessed into the shroud increasing the orifice size and decreasing the gas exit velocity. On nozzle 3 the bio-oil tube was pressed hard against the outer shroud; this only allowed the oxygen to flow through the recessed cuts on the bio-oil tube.

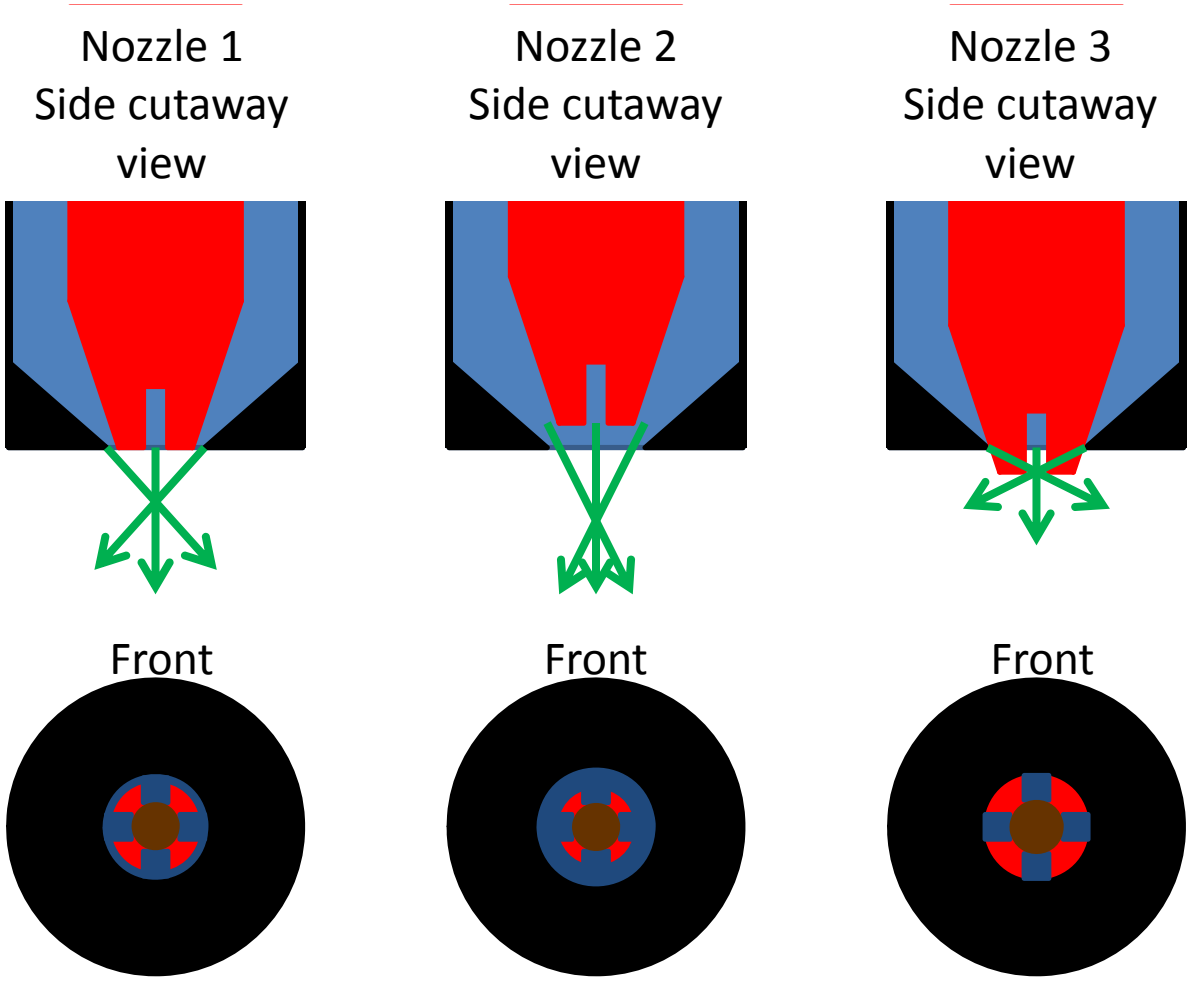

Figure 5 Relative nozzle positions for used for all bio-oil gasification test run on the Iowa State University bio-oil gasification system

The gasification section of the system consisted of four parts. The four sections were the silicon carbide, cable heater, high density insulation, and the stainless steel pressure vessel. Silicon carbide was selected due to its proficient thermal conductivity while it resists secondary chemical reaction. The most critical property of the silicon carbide was its low thermal expansion. As the silicon carbide was exposed to high temperatures and contained within a nonexpanding steel pressure vessel the thermal expansion had to be controlled as to reduce an interference between the two components. A 3600 watt electrical cable heater equipped with an imbedded thermocouple was used to provide adiabatic conditions within this gasifier. The 120 inch cable heater was wrapped around the outside of the 40 inch long, 1.5 inch diameter silicon carbide tube in the shape of a helix. The internal heater provided power for starting the gasification experiments and additionally it minimized the heat loss in the system during operation. The silicon carbide and cable heater are covered with multiple layers of high density Kaowool® ceramic insulation. The combination of silicon carbide, the cable heater and insulation was then slid into the stainless steel pressure vessel.

Figure 6 Iowa State University bio-oil gasification reactor

A heat transfer thermal circuit was constructed to determine the amount of insulation needed and in-turn the size of the pressure vessel. The assumptions were made that the cylinder surface was acting as a gray body where α was equal to ε to simplify the radiation portion of the heat transfer circuit. To complete the thermal circuit shown in figure 7 some assumptions had to be made. A worst case scenario was chosen in which the heater and room were fixed at 1000^{o}C and 25^{o}C respectively and a pressure vessel surface temperature was targeted at 50^{o}C. The resulting showed that 2 inches of the high density insulation would reduce the temperature of a stainless steel vessel to around the target 50^{o}C. When adding

the 1.5 inch diameter silicon carbide tube with the 2 inches need for insulation, the resulting pipe size was 6 inch nominal pipe.

$$\therefore \quad \frac{(T_{Heater} - T_{Room})}{R_{total}}$$

$$R_{Total} = R_{Insulation} + R_{Steel} + \frac{1}{\frac{1}{R_{Convection}} + \frac{1}{R_{Radiation}}}$$

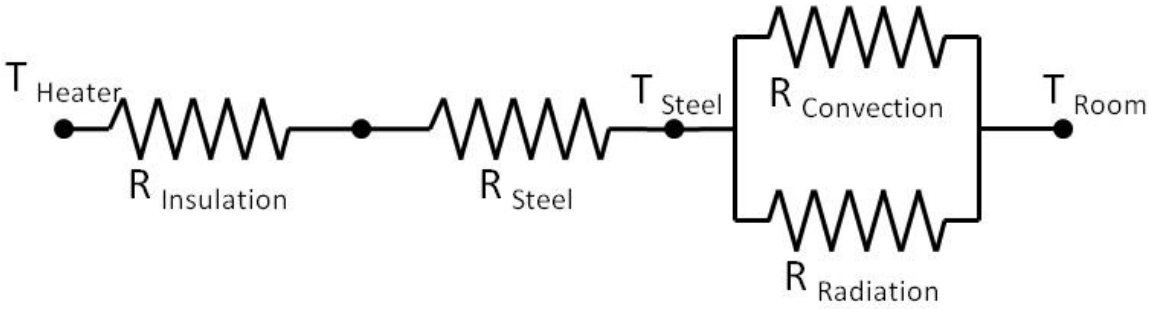

Figure 7 Heat transfer equations and thermal circuit used for sizing the gasification reactor

The ASME B31.3-2008 pressurized pipe codes provided the maximum allowable stress in 316 stainless steel pipe verses the temperature of the metal. If a pressure vessel designed to operate below the maximum allowable stress line plotted in figure 8, the vessel is deemed safe to operate. A point was plotted on the graph in figure 8 representing the operational point of this reactor. A factor of safety of 4 was applied to the 50^{o}C surface temperature calculated above resulting in a 200^{o}C surface temperature rating. In conjunction, hoop stress calculations were completed on a 6 inch, schedule 80 pipe containing 700 psig of pressure. This operation point gave a factor of safety of 2.5 below the stress curve and resulted in a pressure vessel diameter of 6 inches.

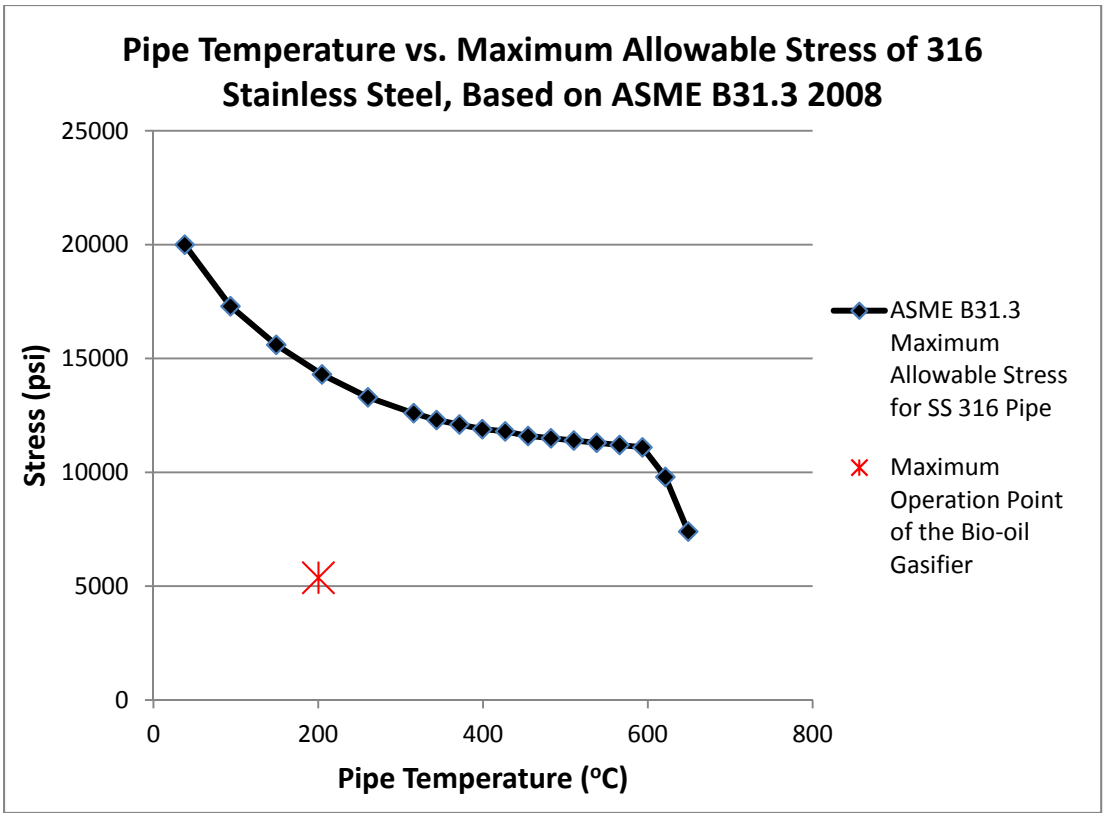

Figure 8 ASME B31.3 2008 Maximum allowable stress verses temperature chart for 316 stainless steel

The 6 inch pipe was capped using 6 inch, 600 pound class, 316 stainless steel pipe flanges based on the ASME B16.5-2003 pipe flange code.

The nozzles discussed above create liquid jets that are sprayed in to the center of the silicon carbide reaction chamber. For all experiments reported in this report the heater set point was 850°C using the Watlow control modules. When the liquid is sufficiently atomized and volatilized the oxygen can act as a reducing agent assisting in breaking the liquid feedstock down into syngas through exothermic reactions. The heat produced from these exothermic reactions was captured using a ten point thermocouple that was inserted down the middle of the reaction chamber. The relative position of each of the ten thermocouples is indicated by figure 9. Each thermocouple position was separated by a distance of 4 inches for the length of the reactor.

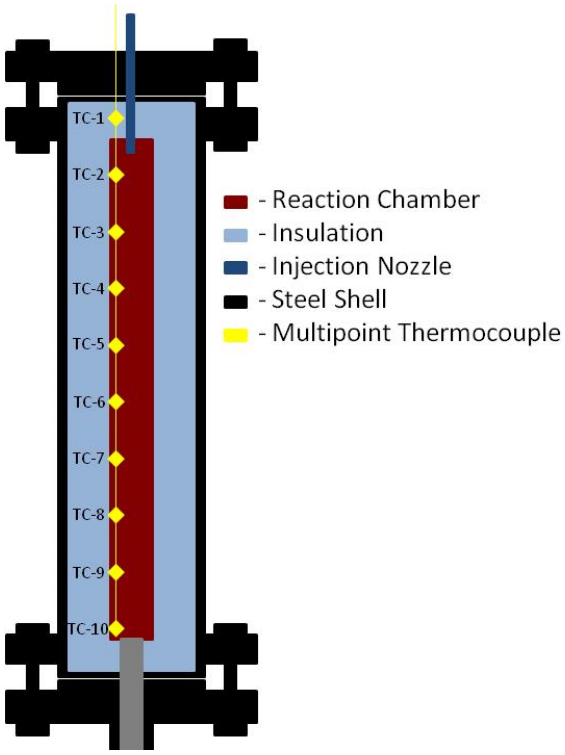

Figure 9 Sectioned gasification vessel with thermocouple locations

The syngas and remaining residue exits the gasifier and travels into the collection system. The collection system is designed to remove tar, char, and water from the syngas. As the tar, char, and water was collected together in all experiments, it will be referred to as reactor residue. The collection system is made from one-inch diameter 316 stainless steel tubing with Swagelok® tube fittings. At the bottom of the this tubing is a collection container that is made from two inch tubing. A water jacket was placed around the collection system using 1/4-inch copper tubing providing a constant temperature heat transfer surface. The targeted exit gas temperature for these experiments was 50^{o}C. The end of the collection tubing was then packed with glass wool to collect any remaining particles that did not drop out due to condensation via impingement.

Figure 10 Iowa State University bio-oil gasification collection system

After the production gas has been cooled, the gas is ready to be analyzed. A slip stream of the syngas was taken and run through a micro gas chromatograph to analyze the molecular composition. The micro gas chromatograph was calibrated using standard known gas composition. Included in the calibration was diatomic nitrogen. As diatomic nitrogen would not be produced during operation of the liquids gasifier it was used to understand the overall flow rates of gases through the micro gas chromatograph. Using a flow meter, one standard liter per minute of nitrogen gas was applied to the liquid gasification system during

experiments. This flow of nitrogen allowed the total volume of syngas to be calculated by using the gas composition recorded and the known calibration curves from the micro gas chromatograph.

The control system consisted of multiple Watlow® logic modules. These modules monitor and control thermocouples, pressure transducers, heaters, valves, motors, and flow meters. These readings are then exported into SpecView, a data acquisition system, to log the data every 5 seconds of operation.

3.6 Analytical Equipment

The following section details the equipment and covers a brief overview of each methodology used by the instruments or analysis techniques.

3.7 Karl Fischer Moisture Titrator

The Karl Fischer (KF) colometric titrator is used to calculate the water concentration in liquids. The KF uses one drop of sample from a 1mL syringe. The syringe is weighed before and after the drop is released into an alcohol based solvent containing sulfur dioxide (SO2), idodide (I-) and imidazole. Once the sample is fully dissolved the KF slowly applies a current through two electrodes to the system to drive the reactions listed below. For each mole of iodide consumed, one mole of water is consumed. Entering the differential mass of the sample syringe in the machine allows it to return the percent water in the sample.

$$ROH + SO_2 + R'N \leftrightarrow [R'NH]SO_3R \qquad \text{Equation (1)}$$

$$H_2O + I_2 + [R'NH]SO_3R + 2R'N \rightarrow [R'NH]SO_4R + 2[R'NH]I \qquad \text{Equation (2)}$$

3.8 Ultimate Analysis (CHNS)

The vario micro cube produced by Elementar America Inc. uses combustion to analyze a sample's elemental composition of carbon, hydrogen, nitrogen, sulfur, and oxygen by difference. A 5mg sample of bio-oil is placed in a tin container with 5mgs of tungsten oxide. Tungsten oxide acts as a heat carrier to vaporize the bio-oil sample quickly and completely. The tin container is then sealed air tight and injected into the micro cube. The sample enters a 1200^{o}C furnace where it is reacted with oxygen to produce

combustion gases N2, CO2, H2O, and SO2. These gases enter a temperature programmed desorption column and are released in-turn to the thermal conductivity detector where the system then calculates the percentage of CHNS resulted from the original sample.

3.9 Thermal Gravimetric Analysis (TGA)

The Thermo Gravimetric Analyzer or TGA uses a microbalance and differential scanning calorimetry to measure changes in mass and heat flux while the sample devolatilizes. The 20mg sample of bio-oil is placed in a ceramic cup and capped using an aluminum lid. The cup is lowered into the TGA and placed on a platinum scale and the lid is then removed. A horizontal furnace encases the cup and scale and is purged with nitrogen gas before the heat cycle is started.

The method used ramps the temperature of the furnace up at 10^{o}C/min until it reaches 105 ^{o}C, then holds the temperature for 30mins to drive off moisture and light volatiles. The furnace is then ramped up to 900^{o}C to determine the total volatiles in the sample. The purge gas is then switched from nitrogen to air to combust the remaining material to determine the ash content. The TGA, also known as approximate analysis, is used to quantify the volatile fixed carbon and ash content.

3.10 GPC

GPC, or gel permeation chromatography, is used to find the molecular weight (MW) distribution across a liquid sample. The liquid sample is prepared by mixing 20 parts tetrahydrofuran (THF) with 1 part bio-oil by volume. The sample is pumped over a specialized column filled with beads with micro pores using the Dionex UltiMate 3000 HPLC pumps. As the solution passes through the column, the smaller particles will have longer residence time than larger particles. Molecular weight sensitive detectors register the concentration of polymers leaving the column over a given time resulting in a molecular weight distribution of the desired sample.

3.11 Bio-oil Density

The density of the bio-oil was tested by using a 5mL syringe and a bench top scale. Each sample was warmed to room temperature and vigorously shaken before a syringe was filled to the 5mL line. A differential weight was then taken for each 1mL of oil removed from the syringe until 1mL remained; providing four sample weights per syringe.

CHAPTER 4 RESULTS

The following section lists the experimental results for the three whole red oak bio-oil samples filtered at 500µm, 90µm, and 40µm screen sizes. All error bars shown represent a 95% confidence interval around the average for a sample population of three within each test.

4.1 Ultimate Analysis and Karl Fischer Moisture Results

The ultimate analysis and Karl Fischer Moisture analysis showed the largest statistical difference of all the lab tests performed on the filtered whole oils. Figure 11 shows that the 90 µm filtered oil resulted in a higher carbon level while showing a reduction in oxygen when compared to the other samples. The 500 µm and 40 µm samples showed no statistical difference when looking at the ultimate analysis. Moisture level showed a significant reduction in the 90 µm and 40 µm samples when compared to the 500 µm filtered oil.

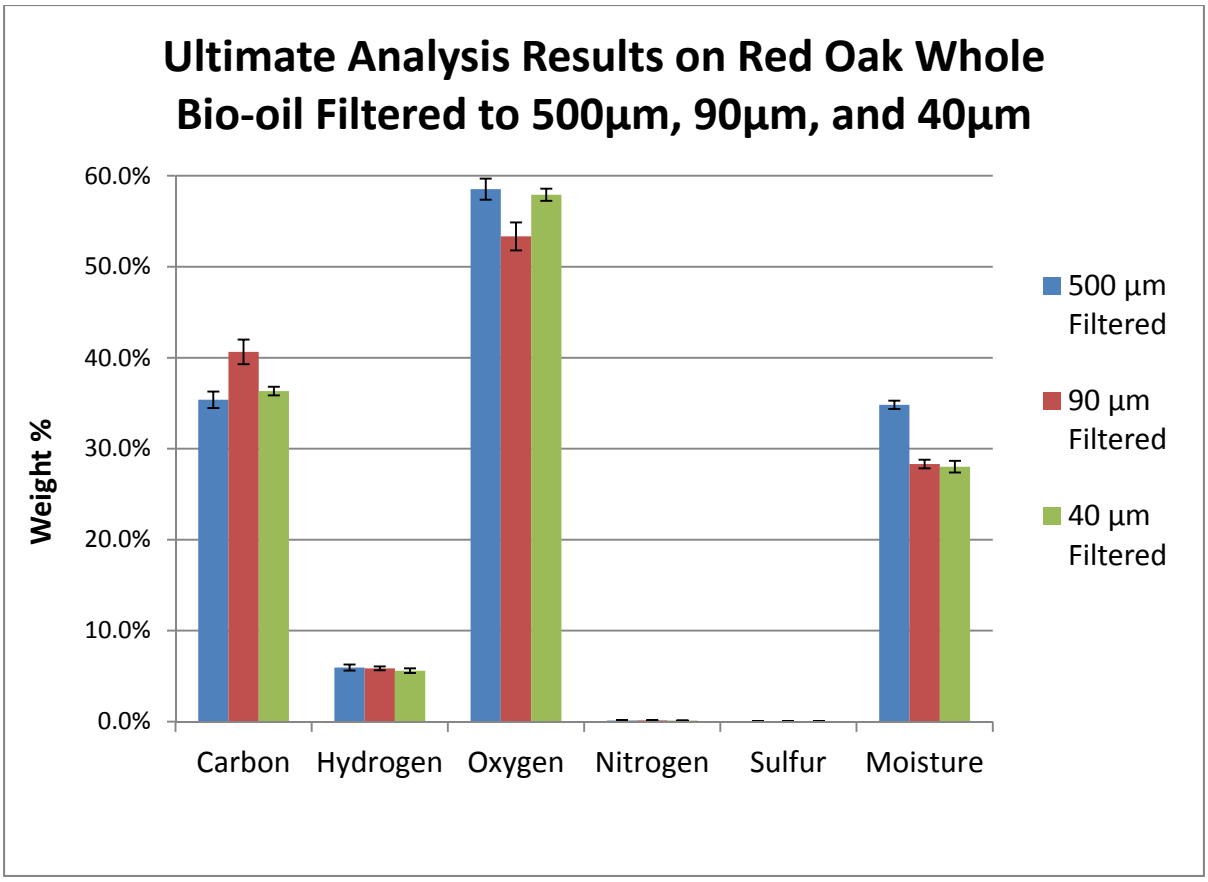

Figure 11 Results of ultimate analysis and Karl Fischer moisture content on whole red oak bio-oil

4.2 TGA Results

No difference was observed in the volatility of the three whole oils as the smallest p-value was much larger then 0.05; thereby there was no statistical difference in results of the TGA data shown in Figure 12.

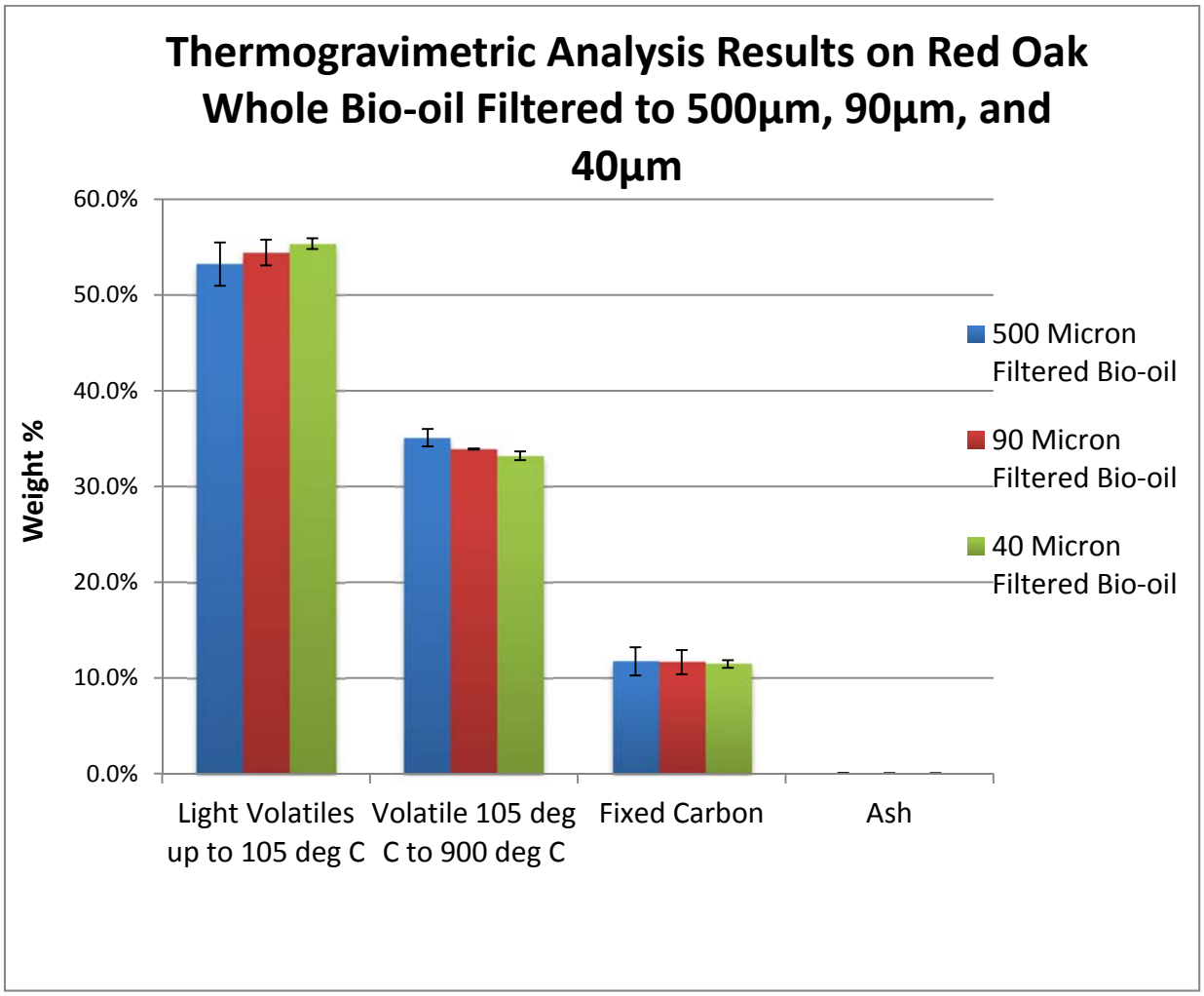

Figure 12 Approximate analysis comparing changes in volatiles, fixed carbon and ash content in filtered whole red oak bio-oil

4.3 GPC Results

The GPC experiment shows a difference in the oils by a shift of the molecular weight content between the 500 µm, 90 µm, and 40 µm samples. Note that the lighter volatile spike is not present in the 90 µm and the 40 µm graphs. The 90 µm sample also shows a shift of increased molecular weight compared to the 500 µm and 40 µm samples.

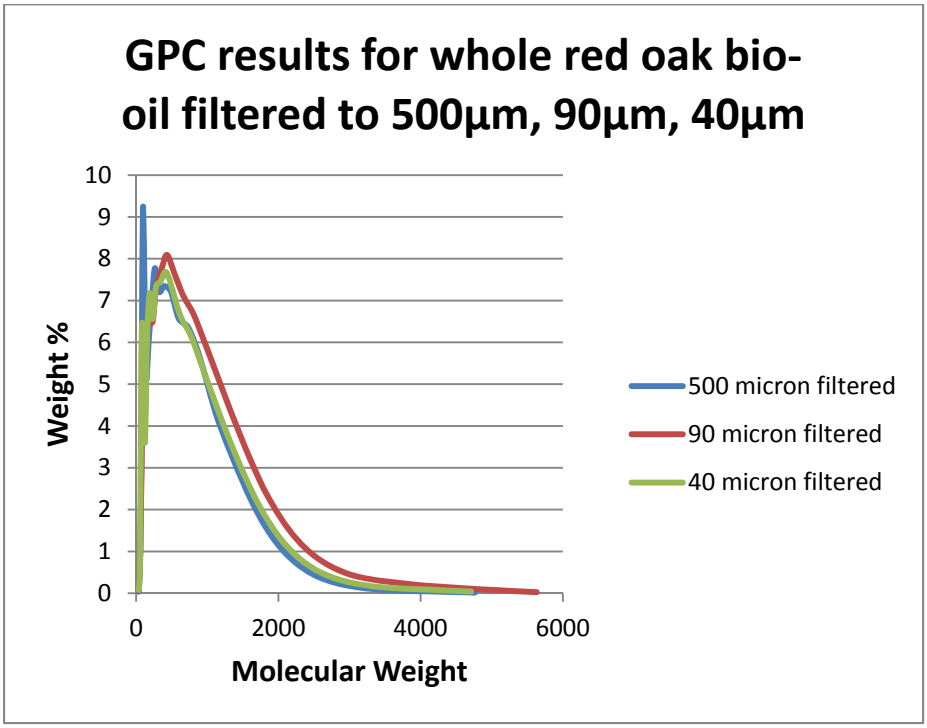

Figure 13 GPC results comparing molecular weight distribution across filtered whole red oak bio-oil

4.4 Density Results

Through the experimental testing of different filtration levels of oil there was no distinguishable difference in whole oil density. (P>0.05 in all cases)

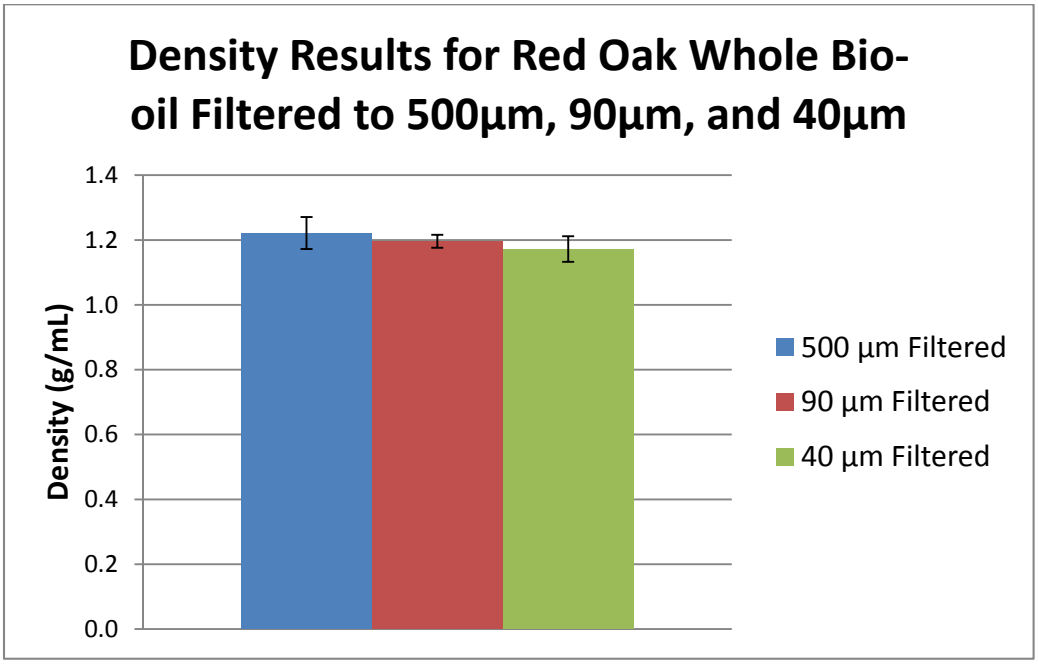

Figure 14 Density results for filtered whole red oak bio-oil

4.5 Methanol Tests:

The gasification of liquid jets system was proven using methanol due to its consistent and clean fluid properties. These tests were compared to the theoretical equilibrium gas composition obtained from the Colorado State University equilibrium calculator [18]. Two tests were run under atmospheric pressure to show repeatability of the system compared to the equilibrium calculations. As shown below, the experimental results conformed closely to the theoretical performance of equilibrium thermodynamics.

Table 4 Syngas composition from atmospheric methanol gasification runs reported in volumetric percent

	H2	CO	CH4	O2	CO2	C2H6	C2H4	C2H2	C3H8
Methanol Test 1	53.6	38.0	0.9	0.0	7.3	0.0	0.1	0.0	0.0
Methanol Test 2	56.6	34.4	0.9	0.0	7.9	0.0	0.1	0.0	0.0
Equilibrium Calculation	59.8	30.5	0.0	0.0	9.6	0.0	0.0	0.0	0.0

An experimental methanol test was conducted at 100 psi_g. This test was correlated to the same equilibrium calculations only at elevated pressure. The carbon dioxide levels recovered from the experimental tests were significantly higher than the calculations predicted, while the hydrogen produced by the system decreased significantly.

Table 5 Syngas composition from 100 psi_g methanol gasification runs reported in volumetric percent

	H2	CO	CH4	O2	CO2	C2H6	C2H4	C2H2	C3H8
Test 3	43.7	26.0	0.7	0.6	29.0	0.0	0.0	0.0	0.0
Equilibrium Calculation	59.8	30.2	6.3	0.0	3.8	0.0	0.0	0.0	0.0

Temperature fluctuations were observed between the atmospheric and pressurized methanol experiments. The atmospheric runs resulted in a consistent reactor temperature profile where the internal thermocouples converged on to a single operating temperature. Conversely, the pressurized run resulted in a divergence from the system set point. As the experimental test proceeded the pressurized run developed a high temperature zone just outside of the system nozzle (TC-3) while the remaining reactor had decreasing temperatures.

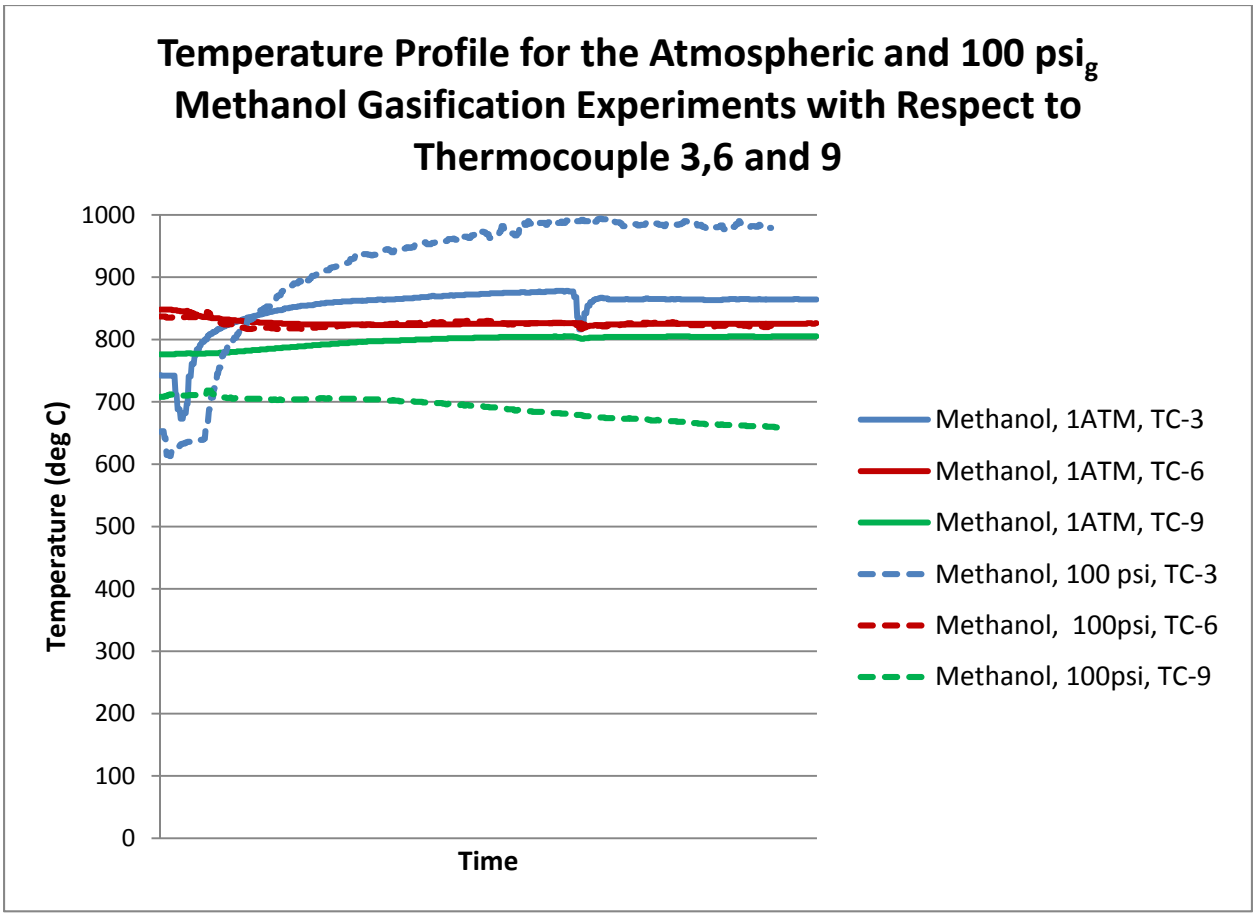

Figure 15 Temperature profile for the atmospheric and 100 psig methanol gasification experiments, monitored thermocouples TC-3, TC-6 and TC-9

4.6 Bio-oil Tests:

Baseline experiments were conducted using nozzle 1 to demonstrate the repeatability of the bio-oil gasification system. This statistical error can then be applied to all the nozzles to determine if there is a significant difference between the nozzle performance. Table 6 displays the syngas composition results with standard deviations and corresponding confidence intervals for three identical tests performed with the nozzle 1 configuration. Similar to the syngas composition the same statistical calculations were applied to the mass balance results.

Table 6 Bio-oil gasification syngas results in volumetric percent for experiments using nozzle 1

Nozzle 1	H2	CO	CH4	O2	CO2	C2H6	C2H4	C2H2	C3H8
Test 1	20.0	41.1	7.8	0.1	27.1	0.3	2.6	0.7	0.2
Test 2	19.5	40.5	7.8	0.1	28.4	0.3	2.6	0.8	0.2
Test 3	20.6	40.4	6.8	0.0	28.9	0.3	2.1	0.7	0.2
Equilibrium Calculation	35.2	41.7	0.0	0.0	12.0	0.0	0.0	0.0	0.0
Average	20.0	40.7	7.5	0.1	28.1	0.3	2.4	0.7	0.2
Standard Deviation	0.6	0.4	0.6	0.0	0.9	0.0	0.3	0.0	0.0
t Distribution for a 95% Confidence Interval	1.4	0.9	1.4	0.1	2.3	0.0	0.8	0.1	0.0

Table 7 displays the total mass recovery, syngas percent, and residue percents by mass for the three identical tests performed with the nozzle 1 configuration.

Using the statistical error calculated above, the syngas compositions from the three nozzle types can be compared side by side, as shown in table 8. The confidence interval calculated in tables 6 and 7 indicates that any change, reported below, results in a statistically significant difference between the three nozzle types in table 8.

Table 7 Bio-oil gasification mass balance results in percent mass for experiments using nozzle 1

Nozzle 1	Over all mass closure	Syngas mass recovered	Residue mass recovered
Test 1	88.8	66.9	28.7
Test 2	86.3	61.2	25.1
Test 3	93.0	61.5	31.4
Average	89.4	63.2	28.4
Standard Deviation	3.4	3.2	3.2
t Distribution for a 95% Confidence	8.4	8.0	7.9

Table 8 Bio-oil gasification syngas results in volumetric percent for experiments using nozzles 1, 2 and 3

	H2	CO	CH4	O2	CO2	C2H6	C2H4	C2H2	C3H8
Nozzle 1	20.0	40.7	7.5	0.1	28.1	0.3	2.4	0.7	0.2
Nozzle 2	17.8	36.8	5.6	0.0	34.8	0.4	1.8	1.7	0.3
Nozzle 3	20.5	43.8	7.2	0.0	23.0	0.2	2.4	1.1	0.1

Table 9 shows the total mass recovery, syngas percent, and residue percentages by mass for all three nozzle configurations.

Table 9 Bio-oil gasification mass balance results in percent mass for experiments using nozzles 1, 2 and 3

	Over all mass closure	Syngas mass recovered	Residue mass recovered
Nozzle 1	89.4	63.2	28.4
Nozzle 2	81.9	34.1	47.8
Nozzle 3	74.8	46.1	28.7

Temperature traces from each of the three nozzles were recorded and plotted below. Thermocouples TC-3 and TC-8 where selected to show the relative difference in how thermal flux reacted to the varying nozzle types; see Figure 9 for TC locations. Nozzle 1 recorded the highest temperatures at the top of the reactor while maintaining controlled level temperatures at the bottom. It was observed that Nozzle 2 started to develop a high temperature zone at TC-3 like Nozzles 1 and 3; however, as time progressed the oil and oxygen mixture resulted in a cooling effect at the top of the reactor. Nozzle 3 showed a temperature profile similar to Nozzle 1 but did not reach as high of a temperature profile. Nozzle 3 also was the only nozzle to show an increase in system temperatures at TC-8.

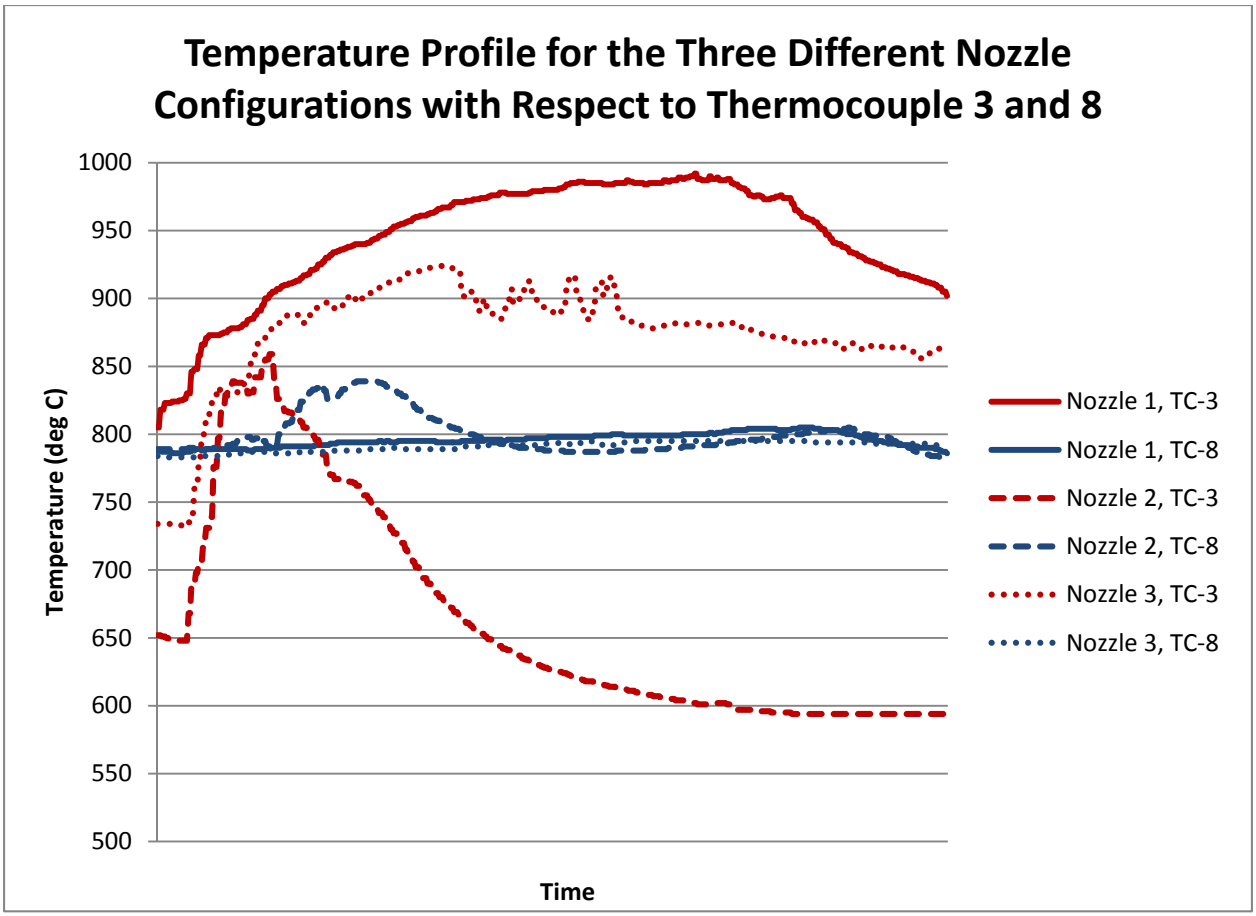

Figure 16 Temperature profile for the atmospheric bio-oil gasification experiments, monitored thermocouples TC-3, TC-8 on nozzles 1, 2 and 3

CHAPTER 5 DISCUSSION

5.1 Whole Bio-oil Filtration

Bio-oil filtration did present several irregularities in the five test experiments performed; however, not all of the experiments show statistical differences between the samples. The density test and TGA tests had potential trends starting with the sample size used, though there was no statistical difference in the samples. ($P>0.05$) An interesting discovery came when looking at the ultimate analysis and moisture content in Figure 11. As the filtration pore size decreased from 500µm to 90µm, the moisture content of the oil also decreased by 5%, but no change was recorded between the 90µm and 40µm oils. Furthermore, the ultimate analysis content was identical between the 500µm and 40µm bio-oil samples but statistically different from the 90µm bio-oil. ($P<0.05$) The average molecular weight graph, in Figure 13, generated by the GPC also shows a shift from high concentration of low MW compounds in the 500µm bio-oil to a broadened higher MW shift in the 90µm oil, followed by a decrease in the higher MW compounds when the oil was filtered further to 40µm.

A hypothesis for the change in moisture content between the samples can result from the processing of the bio-oil. During the filtration process, the bio-oil is heated to 60^{o} C for an extended period of time while being pumped through the filters. During this time, water vapor was observed to be driven off of the bio-oil during the heating process causing the decrease in moisture content between samples. The ultimate analysis shows a statistically significant increase in carbon content and a decrease in oxygen content of the 90µm filtered bio-oil ($P<0.05$), however the hydrogen concentration remained constant. Consequently, there is more occurring between samples than simply moisture reduction. The ultimate analysis showed no difference between the 40 µm sample and the 500 µm sample. ($P>0.05$) This can be a result of the correlation between the decrease in filter size and the reduction of carbon content, coincidentally making the two oil samples appear statistically identical. The GPC experiment shows that there is a difference in the filtered oils by the shift the MW content. This theory can be disproven by the

insignificant change of carbon content in the TGA data; however, more tests are needed to validate any further hypotheses of these results.

Iowa State University's process for producing whole bio-oil is different than a conventional system. The process development pyrolyzer is designed for collecting bio-oil in multiple fractions and it succeeds at this very well. To produce a filtered whole bio-oil, a series of manual steps must be taken and requires extensive heating and agitating of the bio-oil to complete. The multiple stage filtration system requiring the bio-oil to be reheated several times introduces a large incongruity to the process resulting in fluctuations in lab results. The discontinuity of results is most likely due to processing rather than the physical filtration of the bio-oil. However, with decreasing filter sizes, one would start to remove long chain polymers and solids that remain after production. If ISU developed a system to collect whole bio-oil, the filtration process could be completed at room temperature and below 1.0 micron screen size. Using this process, analytical chemistry could be used to show definitive differences among the bio-oil samples.

5.2 Methanol Gasification

The methanol tests were performed to prove the overall concept of gasification of liquid jets. Three tests were performed; two at atmospheric pressure and one at 100 psi_g. All of these tests were compared to equilibrium results preformed on the Colorado State University equilibrium calculation tool. It was found that the liquids gasifier operated seamlessly at atmospheric pressures while using methanol as an ideal fuel source. The results of both atmospheric tests aligned closely to the equilibrium results. Divergences started to occur when the system was pressurized. The calculated pressure run showed that little change was to be expected from the atmospheric runs; however, the experiment showed a different result. Operating the liquid gasifier at 100 psi_g resulted in a dramatic reduction in hydrogen content and a large increase in carbon dioxide.

The temperature profiles further paint the picture that during the pressurized run the system experienced a large exothermic zone near the injection nozzle. It was hypothesized that this zone was due

to poor atomization of the methanol. If the methanol was only partially atomized, the oxygen in the system would only have a portion of the fuel to react with. This decrease in available reaction area would then artificially drive the stoichiometric balance closer to combustion than gasification. Combustion reactions would result in higher temperature profiles and a large increase in carbon dioxide.

The hypothesis for this discrepancy is that the increase in pressure without changing the geometry of the nozzle resulted in a lower pressure drop across the exit of the nozzle. This pressure drop is the driving force that allows for high speed gases to help atomize the liquid fuel. Therefore, to adequately gasify a liquid you must have good volatilization and atomization. As the volatility of the methanol fuel was relatively constant between low pressure and high pressure experiments, the decrease in gasification reactions was driven by the reduction in atomization. Due to this result found on the methanol, it was decided to test the effects of nozzle configuration in combination with the liquid bio-oil to determine the effects of atomization in a gasifier with a liquid that is less volatile then methanol.

5.3 Bio-oil Gasification

Three qualitative nozzles were developed for testing in correspondence with bio-oil. Nozzle 1 was used to perform three baseline experiments. These three tests allowed for an average, standard deviation, and a 95% confidence interval to be created against the variation in experiments. The syngas results showed high correlation between the three tests resulting in 1% or smaller 95% confidence interval windows, while the mass balance data had a higher degree of error of 4%. This variation was then used to evaluate the changes in results found while operating the bio-oil gasifier with all three nozzles.

The syngas results for all three nozzles show a significant difference between nozzles 1 and 2, and 2 and 3; however, there was only minor change between nozzles 1 and 3. Most notably the hydrogen and carbon monoxide decreased while carbon dioxide content increased with decreasing atomization between nozzles 1 and 2. All p-values were less than 0.05 when comparing hydrogen, carbon monoxide and carbon dioxide between nozzle one and two. This comparison further reinforces the idea that decreased atomization will result in localized combustion reactions decreasing the gasification products

H_2 and CO, and increasing the combustion products CO_2 and H_2O. Further signs of reduced reactivity are shown by the increase in recovered residue, as shown in table 9. Nozzle 2 did show a significant decrease in the overall mass balance, however the reduction in overall mass balance was over shadowed by the increase in residue. ($P<0.05$)

Examination of nozzles 1 and 3 results showed the overall performance was similar to each other in many aspects. The hydrogen levels showed no statistical change while the CO levels slightly increased while decreasing the CO2 concentration. ($P>0.05$) Again this reinforces the idea that increased atomization with constant volatilization will result in reactions that behave closer to a well mixed system. The mass balance between nozzle 1 and 3 shows there was statistically the same amount of system residue produced while the resultant syngas created was greatly diminished, in turn reducing the overall mass balance of nozzle 3. This reduction in gas volume is attributed to a small leak that was found after the experiment was completed.

The most evident change between nozzles was observed during operation by monitoring a high temperature zone just after the injection nozzle at TC-3. Figure 16 shows the relative changes in temperature profiles during the operation of each of the nozzles. Nozzle 1 produced a highly exothermic reaction just outside of the nozzle while maintaining constant temperature lower in the reactor. The expectation was that due to the highly exothermic zone on nozzle 1 the CO2 generation would be high, indicating increased combustion; however, this was not observed. Due to the reduced volatility the bio-oil needed the high temperature reduction zone in order to brake the oils into gases so the series of gasification reactions could take effect and shift the resultant gases in to syngas. This was further reinforced when looking at the temperature profiles of Nozzles 2 and 3.

Nozzle 3 mimicked the performance of Nozzle 1; however, the lower temperature at TC-3 and the increase in temperature at TC-8 indicates that exothermic reactions were taking place the full length of the reactor. It was also noted that Nozzle 3 created the most sustainable high temperature zone during operation.

Nozzle 2 did reach a steady state temperature limit, but it did not have the pressure drop it needed to create the sheer force to atomize the bio-oil. Without this critical mixing affect the oil and oxygen did not have enough time to react and create the exothermic reactions needed to promote a sustained gasification reaction. This nozzle combination caused the reaction zone to start at the top of the reactor and slowly move down the reactor. It was predicted due to poor atomization, bio-oil was building up on the walls and slowly volatilized as it interacted with oxygen. This slow volatilization requires energy, therefore the temperature throughout the reactor gradually fell as more and more bio-oil built up on the walls. When the reactor was disassembled the silicon carbide tube with filled with coke as predicted.

CHAPTER 6 CONCLUSIONS

The Iowa State University bio-oil gasification unit demonstrated that continuous gasification of liquid jets is possible. However, the results show that care must be taken when designing the liquids injections system.

The methanol tests proved the functionally of Iowa State University's bio-oil gasifier. The pressurized run, using methanol, indicated that nozzle design was critical for successful gasification. A series of nozzles were developed to exploit the variation of gas exit velocities to show the resulting differences in bio-oil gasification experiments.

The test results from the filtration study proved that the particulate matter could be removed from the bio-oil without drastically effecting the overall composition of the bio-oil. The removal of high molecular weight compounds reduced the probability for the injection nozzle from being clogged during operation and provided a consistent fuel for the bio-oil gasification trials. Future work needs to be completed on bio-oil filtration from a pyrolysis unit that collects bio-oil in a single fraction and does not require heated open barrel mixing. Additionally, attention should be given to filtering the bio-oil below 40micro meters; oils filtered below 40micro meters allows for smaller, more intricate nozzles to be developed for future high pressure gasification experiments.

The qualitative nozzles allowed for quantitative results to be gathered on the effects of atomization in a liquids gasifier. The nozzles showed that the velocity reduction of injected oxygen directly reduced the capability of the gasifier. This was demonstrated by the degradation in the syngas composition and in the increase in collected residue from nozzle 2 with comparison to the other nozzles. Conversely, the increase in the velocity between nozzles 1 and 3 did not show an increase in gasification performance. This indicated that a performance plateau could be achieved, where increased gas velocity does not significantly increase the atomization of the injected liquid.

Future work for this gasification system should identify a nozzle design for atmospheric bio-oil gasification. With the nozzle, the exit gas velocity can be calculated and adjusted for pressure differentials. This will then allow for a scalable design that will account for system pressure increases.

Therefore, the optimized nozzle that allows for a fully developed design of experiments can, in turn illustrate the full capability of a bio-oil gasification system.

Bibliography

[1] Wright M.M., R.C. Brown, A.A. Boateng, Distributed Processing of biomass to bio-oil for subsequent production of Fischer-tropsch liquids: Biofuels Bioproducts Biorefing; Modeling and Analysis, pgs 229-238, 2008

[2] Brown, Robert. *Biorenewable Resources Engineering New Products from Agriculture.* Ames: Blackwell Publishing Professional, 2003. Print.

[3] Rasjvanshi A.K., Biomass Gasification: "Alternative Energy in Agriculture," Vol. II, Ed. D. Yogi. Goswami, CRC Press, pgs. 83-102, 1986

[4] Ciferno J.P., J.J. Marano, Benchmarking Biomass Gasification Technology for Fuels, Chemicals and hydrogen Production: U.S. Department of Energy National Energy Technology Laboratory, June 2002

[5] Tanksale A., J. N. Beltramini, G. M. Lu, A Review of Catalytic Hydrogen Production Processes from Biomass: Renewable and Sustainable Energy Reviews 14, pgs. 166-182, 2010

[6] Cen K., Q. Cehn, X. Cao, Z. Luo, Q. Mei, H. Zhao, J. Zhou, Biomass-oxygen gasification in a High-temperature Entrained-flow Gasifier: Biotechnology Advances, April 2009

[7] Courson C., E. Makaga, C. Petit, A. Kiennemann, Development of Ni Catalysts for Gas Production from Biomass Gasification Reactivity in Steam-and Dry-Reforming: Catalysts Today, Volume 63, Issue 2-4, December 2000

[8] Lv P., Z. Yuan, C. Wu, L. Ma, Y. Chen, N. Tsubaki, Bio-syngas Production from Biomass Catalytic

Gasification: Energy Conversion and Management 48, December 2004

[9] Babu S. P., Biomass Gasification for Hydrogen Production Process Description and Research Needs: Gas Technology Institute

[10] Zhao B., Development of a New Method for Evaluating Cyclone Efficiency: Chemical Engineering and Processing 44, August 2004

[11] Rossum G. V., S.R.A. Kersten, W.P.M. van Swaaij, Catalytic and Noncatalytic Gasification of Pyrolysis Oil: Industrial and Engineering Chemistry Research, March 2007

[12] Pyrolysis Oil Application: Bio Technology Group, http://www.btgworld.com/index.php?id=23&rid=8&r=rd

[13] Megaritis A., Y. Zhuo, R. Messenboch, D. R. Dugwell, R. Kandiyoti, Pyrolysis and Gasification in a Bench-Scale High-Pressure Fluidized-Bed Reactor: Energy and Fuels, 1998

[14] Brown J. N., R. C. Brown, T. J. Heindel, D. R. Raman, Development of a Lab-Scale Auger Reactor for Biomass Fast Pyrolysis and Process Optimization Using Response Surface Methodology, August 2009

[15] Svoboda K., M. Pohorely, M. Hartman, J. Martinec, Pretreatment and Feeding of Biomass for Pressurized Entrained Flow Gasification: Fuel Processing Technology 90, pg. 629-635, 2009

[16] Sakaguchi M., A. P. Watkinson, N. Ellis, Steam Gasification of Bio-oil and Bio-oil/Char Slurry in a Fluidized Bed Reactor: Energy&Fuels 24, pg. 5181-5189, August 2010

[17] Broer, K. M., P. J. Woolcock, P. A. Johnston, R. C. Brown, Steam/oxygen gasification system for the production of clean syngas from switchgrass: Fuel 140, pg. 282-292, 2015

[18] Department of Chemical And Biological Engineering, Colorado State University, David Dandy ©2015, http://navier.engr.colostate.edu/~dandy/code/code-4/index.html